Charging, aggregation, and aggregate strength of humic substances in the presence of cationic surfactants: Effects of humic substances hydrophobicity and surfactant tail length

Azizul Hakim[1,2], and Motoyoshi Kobayashi[3]*

1. Graduate School of Life and Environmental Sciences, University of Tsukuba, 1-1-1 Tennoudai, Tsukuba, Ibaraki 305-8572, Japan
2. Department of Soil Science, University of Chittagong, Chittagong-4331, Bangladesh
3. Faculty of Life and Environmental Sciences, University of Tsukuba, 1-1-1 Tennoudai, Tsukuba, Ibaraki 305-8572, Japan

*Corresponding author, email: kobayashi.moto.fp@u.tsukuba.ac.jp

Conflict of interest

The authors declare that they have no conflict of interest associated with this article.

Abstract

The binding of natural organic matters (NOM) with organic cations and resulting changes in charging and aggregation of NOMs are important in water science and technology such as the enhanced settling by flocculation and the fate control of contaminants. We measured the electrophoretic mobility and aggregate strength of humic substances (HSs), Suwannee river fulvic acid (SRFA) and Leonardite humic acid (LHA), in the presence of cationic surfactants, cetylpyridinium chloride (CPC) and dodecylpyridinium chloride (DPC), to clarify the effects of carbon content, aromaticity of HSs, and the tail length of cationic surfactants on the charging and aggregation. Both of HSs showed charge reversal in the presence of 0.1 - 0.3 mM CPC and LHA in 1 and 2 mM DPC. The iso-electric point (IEP) pH of LHA-CPC and SRFA-CPC system was higher than that of LHA-DPC system, though more DPC concentration was needed for the charge reversal of LHA in DPC. We also observed pronounced aggregation of both HSs in CPC systems around IEP pH, though LHA in higher DPC concentration showed wider range of aggregation pH including IEP pH than the range at low DPC concentration. The maximum strength of LHA aggregate was higher, around 27.6 nN in LHA-CPC system and 19.1 nN in LHA-DPC system, than that of 5.2 nN in SRFA-CPC system. This higher value of aggregate strength in LHA-CPC system than others indicates more hydrophobic interaction in LHA-CPC system. The maximum strength around IEP pH in all the systems indicates the presence of electrostatic interactions along with hydrophobic and other non-DLVO forces.

Key Words: Natural organic matter; Aromatic content; Carbon content; Aliphatic chain length; Flocculation; Floc strength

1. Introduction

The aggregation behavior of humic substances (HSs) along with its charging is a matter of concern in recent days due to its availability and surface activity in natural environmental condition. Though low concentration of these polymeric organic acids is difficult to be separated from water environment [1], several coagulation techniques by using inorganic salts [2], [3], [4] are used to isolate the HSs from water environment. The coagulation and removal of humic acids and natural organic matter (NOM) in the presence of organic molecules and ions are also presented in many literatures [5], [6], and [7]. The binding of ions and/or aggregation of humic substances were proposed by many previous investigations showing different mechanisms of electrostatic and hydrophobic interactions, hydrogen bonding, supramolecular associations, and intramolecular or intermolecular association due to conformational changes [8], [9], [10], [11], [12]. The strength of HSs aggregates and/or flocs depends on pH and shear conditions [13], [14], [15]. Some investigations evaluated the aggregate strength using alum coagulant and expressed the strength as force per unit area at the plane of rupture and found the maximum 0.42 Nm^{-2} [16] and 0.58 Nm^{-2} [17]. They proposed charge neutralization and bridging flocculation are the possible mechanisms of higher aggregate strength. Some other studies focused on the evaluation of the strength of HSs aggregates using alternate shear and measured the strength factors from breakage and regrowth before and after shear [15], [18], [19], and [20].

In recent days, the cationic surfactants especially, the *n*-hexadecyl- or cetylpyridinium chloride (CPC) and *n*-dodecylpyridinium chloride (DPC) are used in daily consumer products and medicine. These surfactants can be discarded to the surrounding soil and aquatic environments as residual or as their by-products [21]. Several studies focused on the aggregation and/or binding of different organic molecules [9], [22], [23], [24], and inorganic ions [25], [26], [27], [28] with HSs.

A few studies focused on the charging behavior and aggregation of HSs in the presence of cationic surfactants [22], [29]. Nevertheless, these investigations did not reveal any numerical value of aggregates strength and did not pay attention to the mechanism determining the strength.

The strength, as a withstanding force against breakup, of flocs/aggregates of polystyrene micro-plastic particles was found to be around a few nN, which is comparable to the adhesion force measured by atomic force microscopy (AFM) [30]. This result suggests that the aggregate strength is directly related to the inter-particle/inter-molecular forces. Chemical force microscopy studies revealed that the inter-molecular adhesion forces depend on the type of molecular groups. The adhesion forces were 28.4 ± 9.4 nN and 4.2 ± 1 nN in -CH_3/-CH_3 (methyl-methyl) and -COOH/-CH_3 (carboxyl-methyl) tip-sample pairs in water, respectively [31]. Some other investigations on the adhesion force measurement by using modified AFM discuss on the dominancy of hydrophobic interaction [32]. These studies found that the adhesion forces of methyl-methyl (CH-CH_3) tip-surface pair interaction in water depend on the length of hydrocarbon chain; 60 ± 5 nN and 12.5 ± 4.4 nN for C_{18} and C_{12} chain length, respectively [32], [33], and [34]. Moreover, a recent investigation on the adhesion properties of alginate hydrogels on self-assembled monolayers (SAMs) terminating with different functional groups proposed that the adhesion behavior of alginate hydrogels is complex, though much higher adhesion force was observed for NH_2-terminated SAMs than CH_3-treminated SAMs [35]. Additionally, they explained the larger pull-off force for NH_2-terminated SAM than hydrophobic SAM is due to the chemical interactions between -NH_2 (amino group) of SAM and -COOH (carboxylic group) of alginate beads, which forms the hydrogen bond and local electrostatic interactions [35]. While these values of adhesion forces can provide insights for the consideration in the strength of

aggregates composed of natural organic matters (NOMs) and other organic molecules, systematic data on the strength of NOM aggregates are lacking.

We have focused on the strength of HSs aggregates in the presence of cationic surfactants, concerning the matter that the aggregates strength affects the removal efficiency and the fate of humic substances along with pollutants [13], [15]. The pH of the system of concern [14], [36] and the hydrophobicity of HSs [9], [29] also affect the coagulation and/or aggregation behaviors of HSs. Therefore, to examine the effect of pH and HS's hydrophobicity on humic acid aggregation, we select Leonardite humic acid (LHA) and Suwannee river fulvic acid (SRFA) with different aromaticity and/or hydrophobicity [9]. Two popular cationic surfactants with quaternary ammonium compounds having different aliphatic tail length DPC and CPC are also selected considering their recent use. This study uses a technique of laminar converging flow to a glass capillary for the breakage [30], [37] of the HSs aggregates to evaluate their strength, focusing on the effect of hydrophobicity of HSs and surfactants on the charging and aggregate strength of HSs as a function of pH. To the best of the authors' knowledge, this is the first experimental result showing aggregate strength in such a complex system of HSs-surfactants focusing the effects of hydrophobicity and surfactants tail length.

2. Materials and Methods

2.1 Materials

We used standard Suwannee river fulvic acid (SRFA) and Leonardite humic acid (LHA) from International Humic Substances Society (IHSS) in this study. The SRFA and LHA powders were dissolved in KOH solution (Wako Pure Chemical Industries) that contained the base amount which is equivalent or more than the amount of carboxylic acid groups of HSs. The subsequent secondary standard (500 mg/L) and experimental HS solutions were prepared by dilution with deionized water (Elix, Millipore) [8], [9].

Two cationic surfactants 1-dodecylpyridinium chloride (DPC) and hexadecylpyridinium chloride monohydrate or cetylpyridinium chloride (CPC) from Tokyo Chemical Industry Co were used. The critical micelle concentration (cmc) of DPC and CPC are 1.52×10^{-2} M and 6.3×10^{-4} M, respectively in water at 25 °C [38]. A previous investigation mentioned the CMC of DPC as a function of temperature [39]. Another investigation showed the Krafft temperature of CPC, which is 11.25 °C [40]. The CMC of CPC is 9×10^{-4} M (0.9 mM) at 20 °C [40] and the CMC of DPC is 1.9×10^{-2} M at 20 °C [41].

These two surfactants were used to examine the effect of tail length and hydrophobic interaction with SRFA and LHA. CO_2 free KOH solution was prepared by following the method by Sipos et al. (2000) [42]. In every new preparation, KCl, KOH and HCl solutions were filtered (DISMIC 25HP 0.2 μm, ADVANTEC) and degassed. Degassing of all the prepared solutions were performed under reduced pressure (GCD-051X, ULVAC) to avoid the CO_2 contamination.

2.2 Methods

2.2.1 Electrophoretic mobility measurements

The electrophoretic mobilities of SRFA and LHA were measured in the presence of both DPC and CPC at 20 °C with a Zetasizer Nano ZS apparatus (Malvern Instruments). We carried out the experiment with 0.2 mM, 1 mM, 2 mM DPC and 0.1 mM, 0.2 mM, 0.3 mM CPC in the presence of 10 mM KCl as function of pH. The 1 mM and 10 mM KCl concentrations were examined in 0.2 mM CPC solution and 1 mM DPC to confirm the effect of KCl concentration. HCl (0.001M and 0.01 M) (JIS special grade chemicals, Wako Pure Chemical Industries) and 0.01 M KOH were used to control the solution pH. The measurements were reproduced in the same experimental condition in some points. Before mixing of all the solutions (water, HCl/KOH, KCl, DPC/CPC solutions with LHA or SRFA), the secondary solutions of LHA (500 mg/L) and SRFA (500 mg/L) were sonicated once for 20 minutes. The HSs (SRFA and LHA) concentration was maintained at 50 mg/L in every measurement of this experiment. A combination electrode (ELP-035, TOA-DKK) was used to measure the pH of the solution.

2.2.2 Macroscopic and microscopic observations of aggregation and dispersion

The observation experiments of aggregation-dispersion of SRFA and LHA solutions in the presence of DPC and CPC were performed in 5 mL prewashed screw-capped polystyrene bottles as a function of pH. To confirm the pH range of SRFA and LHA aggregation in the selected concentration of DPC and CPC, we mixed water, KCl, HCl/KOH, CPC/DPC and SRFA/LHA in every case of visual observations setup. The observation experiments with naked-eyes were performed in 1 mM DPC and 0.2 mM CPC at 10 mM KCl concentration as a function of pH in a series of 5 mL solutions of 50 mg/L SRFA and LHA. Immediately after mixing, the suspensions in the bottles were turned over from upright to normal position once and then left stand for 24

149 hours. Then the macroscopic pictures were taken to observe the range of pH for the aggregation
150 after 24 hours. The aggregated suspension was also observed through a microscope (Shimadzu
151 BA210E, Moticam 580INT) after 24 hours of the mixing. The microscopic observation was done
152 to infer the approximate size and arrangements of aggregates under different pH condition.

153 **2.2.3 Aggregate strength from breakup of aggregates in a converging flow**

154 We used the similar experimental setup as in the previous literatures [8], [30], [37], [43],
155 [44], [45] [46]. A schematic illustration of the experimental setup and instrument is shown in the
156 supporting information (Figure S1). In this experiment for the breakage of HSs aggregate, we used
157 a converging flow into a glass capillary of 0.8 mm inner diameter at 10 mL/min volumetric flow
158 rate using a syringe pump (Fusion 200, Chemyx). The aggregated suspension was taken from the
159 bottle of macroscopic study after 24 hours of observation for the breakage experiment.

160 After the flow of the aggregated suspension through the capillary, we observed the broken
161 aggregates in the capillary, which was immersed in water in the O-ring between a glass slide and
162 a glass cover to reduce the optical distortion, through a light microscope. We then captured the
163 image focusing on the maximum size of broken SRFA and LHA aggregates. We used ImageJ
164 software (ImageJ 1.51K) to calculate the major and minor axes (d_{maj} and d_{min}) of the best-fit ellipse
165 of the maximum sized aggregate from the captured images, because the aggregates behavior in the
166 flow fields can be approximated as ellipsoids [43], [44]. A room temperature was 20 °C throughout
167 the total measurements.

168 The aggregates in flow fields can be broken down when the hydrodynamic rupturing force
169 F_{hyd} acting on the aggregates exceeds the aggregate strength $F_{aggregate}$,

170 $$F_{hyd} \geq F_{aggregate}. \quad (1)$$

So, the aggregate strength is reflected by the maximum sized aggregates after breakage and thus $F_{hyd} = F_{aggregate}$. The observation of Higashitani et al. (1991) [45] and Blaser (2000a) [43] deduced that the breakage of the flocs/aggregates caused by the extremely high elongation rate occurs at the proximity of the capillary tube during the entrance in the converging flow. The highest elongation rate of flow, $A_{c,max}$, along the centerline in the converging flow into the capillary tube with a volumetric flow rate of Q and a radius R determines the maximum aggregate size. That is, [30], [37], [47]

$$A_{c,\max} = \frac{3\sqrt{3}Q}{32\pi R^3} \qquad (2)$$

In the field of an axisymmetric straining flow with an elongation rate, A, the hydrodynamic rupturing force acting on the ellipsoidal SRFA and LHA aggregates of surface area S, can be calculated by the equation from Blaser (2002) [47].

$$F_{hyd} = C_{hyd} S \mu A / 2 \qquad (3)$$

where μ is the viscosity of fluid, and the values of C_{hyd}, which depends on the ratio d_{maj}/d_{min}, are listed in the previous literature of Kobayashi (2005) [37]. We always focus on the maximum surface area of SRFA and LHA aggregates, S_{max}, which can be calculated by using the major and minor lengths (d_{maj} and d_{min}) of the fitted ellipses extracted from ImageJ and substituted in the following equation [48].

$$S = 2\pi\left(a^2 + \frac{ac^2}{\sqrt{c^2 - a^2}} \arccos\frac{a}{c} \right) \qquad (4)$$

where $2a=d_{min}$, $2c=d_{maj}$.

The aggregate strength calculation was done by following the methods described in the previous literature [30], [37]. Kobayashi (2004) [30] deduced the following equation to calculate the strength of aggregates considering that the flow along the streamlines is subjected to the higher stress

$$F_{aggregate} = (C_{hyd} S)_{\max} \mu A_{c,\max} / 2 \qquad (5)$$

where, $F_{\text{aggregate}}$ aggregate strength, $S_{\max}$ maximum surface area of the aggregate as an ellipsoid, $A_{\text{c,max}}$ highest elongation rate of flow along the centerline of the converging flow.

3. Results and Discussion

3.1 Electrophoretic mobility of humic substances (SRFA and LHA) in the presence of CPC and DPC

3.1.1 Electrophoretic mobility in CPC solutions

We measured the electrophoretic mobility of SRFA and LHA in the presence of CPC in KCl solution as a function of pH. The electrophoretic mobility of SRFA and LHA at 0.1 mM – 0.3 mM of CPC are presented in Figures 1 and 2. 10 mM KCl solution was used in every concentration of CPC solution in SRFA and LHA solutions, with mobility data at 1 mM KCl and 0.2 mM CPC concentration. The SRFA and LHA show charge reversal in all the experimented concentrations of CPC at 10 mM and 1 mM of KCl. The iso-electric point (IEP) pH of SRFA and LHA shifts towards a higher pH value with the increase of CPC concentration from 0.1 mM to 0.3 mM. There is a gradual decrease of the absolute positive electrophoretic mobility to charge neutralization with the increase of pH. With the increase of CPC concentration, the charge reversal can be observed within a wide pH range. This indicates a possibility of more adsorption and binding with the increase of CPC concentration.

The electrophoretic mobility of SRFA and LHA shows no noticeable difference at 1 mM and 10 mM of KCl in 0.2 mM CPC solutions, though IEP shifts toward a higher pH value in LHA than that of SRFA. In comparison between the SRFA-CPC and LHA-CPC systems, the IEP pHs are around 5.3 and 6.4 in 0.2 mM CPC at 10 mM KCl for SRFA and LHA, respectively. We also find the higher magnitude of electrophoretic mobility in the charge reversed pH for LHA than that of SRFA at pH around 3 in 0.2 mM and 0.3 mM of CPC solutions. These higher absolute positive

values of electrophoretic mobility at low pH and shifting of IEP towards a higher pH for LHA indicate the effect of more hydrophobic interaction of LHA-CPC than that of SRFA-CPC system.

The hydrophobic interactions and its effect on the charging behaviour of humic substances were discussed in many previous literatures [9], [29], [22]. That is, the more interaction and binding of CPC with LHA than that of SRFA with CPC. The SRFA has less carbon and aromatic groups [9] than that of LHA, indicating the more aromatic and/or hydrophobic groups interact in LHA-CPC system. The imperceptible effect of KCl in this investigation is comparable with the proton binding behaviour of humic substances in KCl solution [23]. That is, the effect of KCl in LHA-CPC and SRFA-CPC systems is not obvious. These phenomena can be explained by the more susceptibility of CPC to LHA and SRFA than that of KCl. Hydrophobic interaction predominates in both system than that of double layer screening by KCl. The trifling effect of KCl solutions on electrophoretic mobility can be explained by the porous and permeable structure of HSs [49]. That is in these systems there is a possibility of the K^+ entrapment and inclusion [23], [49] in the humic acid and has imperceptible effect on mobility.

3.1.2 Electrophoretic mobility in DPC solutions

The Electrophoretic mobility of LHA was also measured in the presence of 0.2 mM to 2 mM DPC in KCl solution (Fig. 3). The LHA shows no charge reversal in 0.2 mM of DPC, though the charge reversal happens at higher concentration of DPC at 1 mM and 2 mM. We observe no notable effect of 1 mM and 10 mM KCl solution at 1 mM of DPC solution in the electrophoretic mobility of LHA. The IEP pH of LHA solution shifts toward higher pH by increasing DPC concentration from 1 mM to 2 mM. The IEPs of LHA are around pH 3.9 and pH 5.8 in 1 mM and 2 mM DPC at 10 mM KCl solution, respectively. This phenomenon of IEP shifting to higher pH

values is due to more adsorption and hydrophobic interaction of LHA and DPC. Similar shift was found in the presence of other hydrophobic ions and molecules with humic acid [9], [22], [29]. The degree of charge reversal and absolute value of electrophoretic mobility at pH 3 are higher in the case of SRFA-CPC and LHA-CPC than that of LHA- DPC system. But the higher IEP pHs of the LHA-CPC system (pH around 6.4) than that of LHA-DPC system (pH around 3.9) indicates more hydrophobic interaction in LHA-CPC system than that of LHA-DPC system, respectively. This higher CPC binding and interaction with LHA can be also explained by the lower solubility of CPC than that of DPC. Although the charge reversal occurs in the higher concentration of DPC in LHA-DPC system, 1 mM DPC needed to induce charge reversal is much higher than that for SRFA-CPC and LHA-CPC systems. The IEP pH in LHA-CPC system is higher than that of IEP pH around 3.9 of LHA-DPC system in 1 mM DPC at 10 mM KCl solution. At pH around 4, the LHA possesses a charge amount around 2.08 meq/g calculated from IHSS data. This 2.08 meq/g of LHA charge is equivalent to 0.1 mM (2.08 mmol/g × 50×10^{-3}g/L) for 50 mg/L of LHA at pH 4. This charge amount is lower than the experimental concentration of 1 mM DPC. This indicates that a part of added DPC are adsorbed to LHA and free DPC molecules remain unbound if the IEP is induced by charge neutralization. The lower magnitude of charge reversal at 1 mM of DPC could also be explained by the higher water solubility of DPC. This higher solubility of DPC and/or shorter alkyl tail length render weaker attraction of DPC to LHA. This solubility related weak attraction was also explained in the previous literature [50].

We also calculated the ratios of added concentrations of CPC and DPC to CMCs of CPC and DPC ($C_{CPC,DPC}$/$CMC_{CPC,DPC}$) and the ratios of added amounts of CPC and DPC to HSs charge amounts ($C_{CPC,DPC}$/charge of HSs) at pH around 6 (Figure S3). These normalized ratios of $C_{CPC,DPC}$/$CMC_{CPC,DPC}$ and $C_{CPC,DPC}$/charge of HSs show no noticeable difference for SRFA and

LHA in CPC (Figure S3 A, B) at pH around 6 at any concentration to charge ratios. Although the charge amount of SRFA and LHA differ at pH around 6, the normalized concentration to CMC shows similar effect. This result indicates that the CPC interacts greater amount with HSs due to CPC hydrophobicity or least solubility than DPC.

3.2 Aggregation-dispersion of Suwannee river fulvic acid (SRFA) and Leonardite humic acid (LHA) in CPC and DPC solutions

We conducted the naked eye observation and microscopic observation of aggregation and dispersion of Suwannee river fulvic acid (SRFA) and Leonardite humic acid (LHA) in the presence of CPC and DPC system in KCl solution. We carried out this experiment under different pH condition (3-10) in the 5 mL polystyrene plastic bottle. The result of macroscopic aggregation dispersion is shown in the pictures of the supporting information (Figure S2). The naked eye observation in the SRFA-CPC and LHA-CPC systems showed that the aggregation is more pronounced in and around IEP pH. The aggregates size and pH range of aggregation in LHA-CPC (pH around 3.9-7.6) and SRFA-CPC (pH around 4.3- 6.8) systems show a clear difference (Figure S2). The pH range of aggregation and size of macroscopic aggregates are larger in LHA-CPC system than that of SRFA-CPC system. The macroscopic pictures show that the LHA-CPC aggregates in 10 mM KCl are darker and more interconnected than SRFA-CPC system in 10 mM KCl solution. The aggregates at designed pH were also investigated under the microscope to compare any structural variability and arrangement depending on pH and humic substances (HSs) with different aromaticity and hydrophobicity. The microscopic pictures of LHA-CPC and SRFA-CPC show the clear comparison of aggregates size and their structural arrangement in different pH (3-10) (Figure 4). In the both SRFA-CPC and LHA-CPC, more pronounced and larger aggregates appear at pH near around IEP than other pH (Figures 4, 5, and S2). Thus, the charge neutralization

289 is required to form larger aggregates composed of humic substances and cationic surfactants. In
290 addition, the HS aggregation is much pronounced for more hydrophobic LHA, demonstrating that
291 hydrophobic moieties of HSs determine the degree of HSs aggregation. Some of the studies
292 demonstrated the poorly formed vesicles type structure formation of SRFA in the presence of
293 cationic surfactants [10]. This type of poorly formed structure resembles our investigation where
294 poor aggregation regime is confirmed beyond the IEP pH (Figure 4 A, C, and D, F). This poorly
295 formed aggregates showing sphere-shaped aggregates and/or particles were also confirmed in soil
296 humic acid and cationic detergents interaction [51]. These previous findings clearly support our
297 outcome of the microscopic observation demonstrated in the Figure 4 A, C, D and F.

298 The macroscopic pictures of aggregation-dispersion of LHA-DPC system are shown in the
299 supporting information (Figure S2). The pH range of aggregation in LHA-DPC system at 10 mM
300 KCl solution increases with the increase of DPC concentration from 0.2 mM to 1 mM (Figure S1).
301 The aggregation is more pronounced at low pH for low concentration of 0.2 mM DPC at 10 mM
302 KCl, whereas with the increase of DPC concentration to 1 mM at 10 mM KCl solution, wider pH
303 range of aggregation from low pH including the IEP pH until pH around 7 (Figure S2). This
304 macroscopic aggregation is supported by microscopic observation of aggregates at different pH
305 (Figure 5). The larger aggregates are formed at low pH, whereas at high pH no more large
306 aggregates are observed except some tiny particulates. This low pH aggregation can be explained
307 by higher hydrophobicity and/ or aromaticity due to low charge of HSs at low pH (Table S2),
308 which induce strong hydrophobic interaction along with some hydrogen bonding and patch
309 attraction. The intermolecular hydrogen bonding originating from the carboxyl hydrogen could be
310 responsible for this low pH aggregation [12]. The HSs do not have smooth surface for uniform
311 charge distribution, rather the charge heterogeneity could be responsible for the charge-patch

attraction trigger the aggregation. This charge-patch attraction was discussed in many previous studies of colloidal aggregation [52], [53].

The increasing concentration of DPC influences the pH range of aggregation in microscopic and macroscopic organization (Figure S2 and Figure 5). The increasing concentration of DPC in LHA shows a wider aggregation pH range with the network like structure manifesting a wider surface availability for aggregation. This phenomenon is clearly supported by the previous investigation that manifested the interaction of colloidal particles and humic substances with cationic detergents [51]. This previous study also manifested the sphere-shaped particles at lower concentration of cationic detergents which disappeared with the increase of concentration. This sphere type tiny particulates are also observed at the lower concentration of DPC for a wide pH range (Figure 5 B and C).

3.3 Suwannee river fulvic acid (SRFA) and Leonardite humic acid (LHA) aggregate strength in CPC and DPC solutions

We obtained the aggregate strength of SRFA and LHA in the presence of CPC and DPC in 10 mM KCl solution (Figure 6). We see the effect of hydrophobicity of humic substances on the aggregate strength from the quantitative comparison of the strength of SRFA and LHA aggregates with CPC at 10 mM KCl inferred in Figure 4 A, C. The aggregate strength of LHA in DPC solution demonstrates the effect of surfactant tail length compared with CPC in LHA (Figure 4).

The aggregate strength of SRFA in 0.2 mM CPC and 10 mM KCl solution shows a maximum strength 5.2 nN at near around IEP pH 6.2. This maximum strength pH shows a shifting toward higher pH value than that of IEP pH. The aggregate strength of SRFA with CPC ranges from around 0.16 nN to 5.2 nN. Meanwhile, the aggregate strength of LHA with 1 mM and 0.2

mM DPC in 10 mM KCl shows higher aggregate strength than that of SRFA-CPC system. The maximum aggregate strength of LHA in 1 mM DPC and 10 mM KCl solution is around 19.1 nN at pH around 3.7. This pH at the maximum strength is around IEP pH 3.9 from electrophoretic mobility (Figure 3 B). On the other hand, the aggregate strength of LHA in 0.2 mM DPC and 10 mM KCl is also higher than that of SRFA-CPC system. This higher aggregate strength of LHA-DPC system is due to the higher hydrophobicity of LHA, indicated from its higher content of carbon and aromaticity, than that of SRFA (Table S2). Additionally, in both LHA-DPC and SRFA-CPC systems, the maximum aggregate strengths are near around IEP pH, indicating that at around IEP pH the electrostatic attraction causes charge neutralization along with other non-DLVO interactions such as charge patch attraction. The effect of HSs hydrophobicity on the aggregation and charging [9] in the presence of monovalent hydrophobic ion clearly distinguished the effect of humic substances hydrophobicity. However other studies evaluate the importance of hydrophobic and electrostatic interactions focusing the effect of humic substances hydrophobicity on the aggregation and charging in different system of humic acid-protein complexation [23], and HSs in the presence of cationic surfactants [22], [29].

The LHA in the presence of 0.2 mM CPC in 10 mM KCl solution shows the maximum aggregate strength around 27.6 nN. This maximum aggregate strength occurs near around IEP pH around 6.2, whereas in the charge reversal pH (pH around 4 to 5) the aggregate strength ranges from around 5.2 nN to 16.2 nN. On the other hand, in the pH around 7.2, where electrophoretic mobility is negative (absolute value > 0.5), the aggregate strength is much lower and around 3.6 nN to 6.2 nN. This condition of aggregate strength demonstrates that the maximum aggregate strength is around IEP. But beyond the IEP, the values of aggregate strength was higher in the range of charge reversed pH than the pH of negative electrophoretic mobility. This maximum

aggregate strength around IEP could be explained by the charge neutralization. Additionally, the higher strength at the charge reversed pH is also because of electrostatic attraction combined with hydrophobic interaction and charge patch attraction.

The values of maximum aggregate strength are also increasing from SRFA-CPC < LHA-DPC < LHA-CPC. This increasing trend of maximum strength is due to the increase of hydrophobic interaction and humic substances hydrophobicity. On the other hand, the increase in aggregate strength LHA-DPC< LHA-CPC can be explained by longer tail length of CPC than that of DPC. The longer tail length of CPC has a higher rate of adsorption on the LHA than that of DPC on LHA.

The foregoing section of this investigation clearly explores the effect of humic substances hydrophobicity and surfactant tail length on the aggregation, charging and aggregate strength of humic substances. Nevertheless, the effect of the aromaticity and/or hydrophobicity was also noticed in an investigation mentioning about the adsorption of natural organic matters (NOM) on hydrophobic carbon nanotubes, showing the strongest effect of aromatic carbon content of NOM in the adsorption behavior [54]. Hakim and Kobayashi (2018) [9] also showed the clear evidence of hydrophobic interaction and the effect of humic substances hydrophobicity on HSs aggregation. Even though the LHA has lower number of chargeable groups than that of SRFA (Table S2) [9], the strength of LHA-CPC aggregates is higher than that of SRFA-CPC aggregates in any pH range. This higher strength of aggregates in LHA-CPC system obviously shows the dominancy of hydrophobic interactions or the effect of humic substances hydrophobicity over the electrostatic interaction. The higher strength of aggregate in this system of concern can be also explained by the supramolecular association [55] and/or intramolecular or intermolecular association of humic substances due to conformation changes [11]. The higher aggregate strength in the case of higher

aromatic and/or hydrophobic LHA accompanied with lower charge is also supported by the study Hakim et al. (2016) [56] and Sugimoto et al. (2017) [57], which indicate the weak charge prevail with the strong hydrophobic interaction. Kobayashi (2005) [37] explored the strength of natural soil aggregates and found the maximum strength 4 nN. In that study Kobayashi (2005) [37] explained this maximum strength is due to the hetero-coagulation caused by attractive electric double layer interactions [58], [59]. But in our investigation, the LHA aggregates in CPC and DPC systems show around 6.9 times and 4.8 times higher strength near around IEP. This higher strength indicates a strong attractive interaction of hydrophobic ions on hydrophobic surfaces. The dominance of hydrophobic effects of HSs charging and aggregation was investigated by Hakim and Kobayashi (2018) [9], who also explained that the increase of humic substances aggregates size is influenced by the hydrophobicity of humic substances itself. Meanwhile, the effect of hydrophobic interaction on the charge reversal of sulfate and carboxylic latex particles and strong adsorption of monovalent hydrophobic cation were also investigated [56], [57]. These investigations drive the possible causes of higher strength of LHA aggregates and obviously explored the effect of humic substances hydrophobicity and hydrophobic interaction in LHA-CPC system. The adhesive forces in different chemical systems and strength of flocs/aggregates are summarized in Table S1. The range of 0.3-60 nN is comparable to the results found in the present study.

As we discuss the adhesion force measurement using AFM, the adhesion force of thiol monolayer with C_{18} is 60 ± 5 nN and higher than 12.5 ± 4.4 nN of C_{12} chain length in methyl-methyl (CH_3-CH_3) tip-surface pair interaction [32], 33], [34]. Some other investigations showed that the size of hydrophobic side groups triggered the surfactant ion binding manifested by measuring the binding constant and Gibbs energy of binding [60], [61]. These previous

404 investigations made our study fruitful and generate the possible causes of higher strength in LHA-
405 CPC system than LHA-DPC system.

406

407 4. Conclusion

408 The charging and aggregation behaviors along with the aggregate strength of two humic
409 substances (HSs) namely Suwannee river fulvic acid (SRFA) and Leonardite humic acid (LHA)
410 were investigated in the presence of cationic surfactants cetylpyridinium chloride (CPC) and
411 dodecylpyridinium chloride (DPC) as a function of pH.

412 We observed the charge reversal of SRFA and LHA in all experimental conditions from
413 0.1 mM to 0.3 mM CPC concentration, whereas the DPC with shorter aliphatic tail length showed
414 no charge reversal of LHA at 0.2 mM of DPC concentration. The IEPs of both HSs (SRFA and
415 LHA) moved toward higher pH value with the increase of CPC concentration and aromaticity
416 and/or hydrophobicity of humic substances (SRFA < LHA). At higher DPC concentration around
417 1 mM and 2 mM, LHA showed charge reversal, and the IEP shifted to a higher pH value from
418 around 4 at 1 mM DPC to around 5.5 at 2 mM DPC. We also observed the effect of KCl
419 concentration (1 mM and 10 mM) in charging at the experimental conditions of 0.2 mM CPC and
420 1 mM DPC and found no notable effect in both LHA and SRFA solutions.

421 The aggregate strength of LHA with CPC and LHA with DPC showed the maximum values
422 around 27.6 nN and 19.1 nN around IEPs (IEP pH were around 6.4 and 3.9), pH 6.2 and 3.7,
423 respectively in the experimental conditions. On the one hand, the maximum aggregate strength of
424 SRFA with CPC was around 5.2 nN around IEP (IEP pH was around 5.3) pH 6.2, though this pH
425 was a little shifted toward higher pH from IEP. The LHA aggregates with CPC and DPC showed

higher strength than that of SRFA aggregates with CPC because of the difference in hydrophobicity and/ or aromaticity of HSs (LHA > SRFA). The maximum and around maximum values of aggregate strength of LHA with CPC differs significantly ($p < 0.05$) from SRFA with CPC. Comparing the effect of the aliphatic tail length of surfactant (CPC > DPC), we found the higher aggregate strength of LHA with CPC than that of LHA with DPC. The maximum strengths of LHA and SRFA with CPC, DPC, and CPC, respectively obtained around IEP pH differ significantly from each other ($p < 0.05$). Further, the effect of DPC concentration on LHA aggregate strengths was also noticed and the effect was significant at $p < 0.001$. In this investigation, the tail length of cationic surfactant shows a clear effect on the aggregate strength. The increase of tail length induces the strong attractive forces due to the hydrophobic interaction and hydrophobicity of humic substances.

The findings of this investigation could be partly able to dissect the mechanisms of maximum aggregate strength, the possible effects of the humic substances hydrophobicity, hydrophobic interactions, and the net charge of HSs-surfactant aggregate. This investigation gives a clear idea of how the hydrophobicity and charge of organic pollutants and dyes affect the removal efficiency of humic substances from water environment and in waste water treatment plants.

Acknowledgements

The authors are thankful to the financial support by JSPS KAKENHI (15H04563, 16H06382, 19H03070)

References

[1] S. Nagao, T. Matsunaga, Y. Suzuki, T. Ueno, H. Amano, Characteristics of humic substances in the Kuji River waters as determined by high-performance size exclusion chromatography with fluorescence detection, Water Res. 37 (2003) 4159–4170, https://doi.org/10.1016/S0043-1354(03)00377-4

[2] B. A. Dempsey, R. M. Ganho, C. R. O'Melia, The coagulation of humic substances by means of aluminum salts, J. Am. Water Work. Assoc, 76 (1984) 141–150, https://doi.org/10.1002/j.1551-8833.1984.tb05315.x

[3] S. Hussain, J. van Leeuwen, C. Chow, S. Beecham, M. Kamruzzaman, D. Wang, M. Drikas, R, Aryal, Removal of organic contaminants from river and reservoir waters by three different aluminum-based metal salts: Coagulation adsorption and kinetics studies. Chem. Eng. J. 225 (2013) 394–405, https://doi.org/10.1016/j.cej.2013.03.119

[4] J. Song, P. Jin, X. Jin, X. C. Wang, Synergistic effects of various in situ hydrolyzed aluminum species for the removal of humic acid, Water Res. 148 (2019) 106–114, https://doi.org/10.1016/j.watres.2018.10.039

[5] B. Bolto, G. Abbt-Braun, D. Dixon, R. Eldridge, F. Frimmel, S. Hesse, S. King, M. Toifl, Experimental Evaluation of Cationic Polyelectrolytes for Removing Natural Organic Matter from Water, Water Sci. Technol. 40 (1999) 71–79, https://doi.org/10.2166/wst.1999.0445

[6] A. Matilainen, M. Vepsäläinen, M. Sillanpää, Natural organic matter removal by coagulation during drinking water treatment: A review, Adv. Colloid Interface Sci. 159 (2010) 189–197, https://doi.org/10.1016/j.cis.2010.06.007

[7] M. Sillanpää, M. C. Ncibi, A. Matilainen, M. Vepsäläinen, Removal of natural organic matter in drinking water treatment by coagulation: A comprehensive review. Chemosphere 190, (2018) 54–71, https://doi.org/10.1016/j.chemosphere.2017.09.113

[8] A. Hakim, T. Suzuki, M. Kobayashi, Strength of Humic Acid Aggregates: Effects of Divalent Cations and Solution pH, ACS Omega 4 (2019), 8559-8567, https://doi.org/10.1021/acsomega.9b00124

[9] A. Hakim, M. Kobayashi, Aggregation and charge reversal of humic substances in the presence of hydrophobic monovalent counter-ions: Effect of hydrophobicity of humic substances. Colloids Surfaces A Physicochem. Eng. Asp. 540 (2018) 1–10, https://doi.org/10.1016/j.colsurfa.2017.12.065

[10] A. A. Chaaban, B. Lartiges, V. Kazpard, C. Plisson-Chastang, L. Michot, I. Bihannic, C. Caillet, B. Prelot, Probing the organization of fulvic acid using a cationic surfactant. Colloids Surfaces A Physicochem. Eng. Asp. 504, 2016, 252–259. https://doi.org/10.1016/j.colsurfa.2016.05.032

[11] R. Baigorri, M. Fuentes, G. González-Gaitano, J.M. García-Mina, Analysis of molecular aggregation in humic substances in solution. Colloids Surfaces A: Physicochem. Eng. Asp. 302 (2007), 301–306. https://doi.org/10.1016/j.colsurfa.2007.02.048

[12] U.D. Jovanović, M.M. Marković, S.B. Cupać, Z.P. Tomić, Soil humic acid aggregation by dynamic light scattering and laser Doppler electrophoresis. J. Plant Nutr. Soil Sci. 176 (2013) 674–679. https://doi.org/10.1002/jpln.201200346

[13] H. Rong, B. Gao, M. Dong, Y. Zhao, S. Sun, Y. Wang, Q. Yue, Q. Li, Characterization of size, strength and structure of aluminum-polymer dual-coagulant flocs under different pH

and hydraulic conditions, J. Hazard. Mater. 252–253 (2013) 330–337, https://doi.org/10.1016/j.jhazmat.2013.03.011

[14] C. Sun, Q. Yue, B. Gao, R. Mu, J. Liu, Y. Zhao, Z. Yang, W. Xu, Effect of pH and shear force on flocs characteristics for humic acid removal using polyferric aluminum chloride-organic polymer dual-coagulants, Desalination 281 (2011) 243–247, https://doi.org/10.1016/j.desal.2011.07.065

[15] D. Wang, R. Wu, Y. Jiang, C.W.K. Chow, Characterization of floc structure and strength: Role of changing shear rates under various coagulation mechanisms, Colloids and Surfaces A: Physicochemical and Engineering Aspects, 379 (1–3) (2011), 36–42, https://doi.org/10.1016/j.colsurfa.2010.11.048

[16] D. H. Bache, E. Rasool, D. Moffat, F. J. McGilligan, On the strength and character of alumino-humic flocs, Water Sci. Technol. 40 (1999) 81–88, https://doi.org/10.1016/S0273-1223(99)00643-5

[17] T. Li, Z. Zhu, D. Wang, C. Yao, H. Tang, Characterization of floc size, strength and structure under various coagulation mechanisms, Powder Technol. 168 (2006) 104–110, https://doi.org/10.1016/j.powtec.2006.07.003

[18] Y. Wang, B.Y. Gao, X. M. Xu, W.Y. Xu, G.Y. Xu, Characterization of floc size, strength and structure in various aluminum coagulants treatment, Journal of Colloid and Interface Science, 332(2) (2009) 354–359. https://doi.org/10.1016/j.jcis.2009.01.002

[19] S. S. Sung, S.P. Ju, C. Hsu, A.S. Mujumdar, D. J. Lee, Floc strength evaluation at alternative shearing with presence of natural organic matter, Drying Technology, 26(8)(2008) 996–1001. https://doi.org/10.1080/07373930802115669

514 [20] W. Z. Yu, J. Gregory, L. Campos, Breakage and regrowth of Al-humic flocs - Effect of
515 additional coagulant dosage, Environmental Science and Technology, 44(16)(2010) 6371–
516 6376. https://doi.org/10.1021/es1007627

517 [21] T. Ivanković, J. Hrenović, Surfactants in the environment, Arh. Hig. Rada Toksikol. 61
518 (2010) 95–110, https://doi.org/10.2478/10004-1254-61-2010-1943

519 [22] L. K. Koopal, T. P. Goloub, T. A. Davis, Binding of ionic surfactants to purified humic acid,
520 J. Colloid Interface Sci. 275 (2004) 360–367, https://doi.org/10.1016/j.jcis.2004.02.061

521 [23] W. F. Tan, L. K. Koopal, L. P. Weng, W. H. van Riemsdijk, W. Norde, Humic acid protein
522 complexation. Geochim. Cosmochim. Acta 72 (2008) 2090–2099,
523 https://doi.org/10.1016/j.gca.2008.02.009

524 [24] M. M. Yee, T. Miyajima, N. Takisawa, Study of ionic surfactants binding to humic acid and
525 fulvic acid by potentiometric titration and dynamic light scattering, Colloids Surfaces A
526 Physicochem. Eng. Asp. 347 (2009) 128–132,
527 https://doi.org/10.1016/j.colsurfa.2009.02.010

528 [25] N. Kloster, M. Brigante, G. Zanini, M. Avena, Aggregation kinetics of humic acids in the
529 presence of calcium ions, Colloids Surfaces A Physicochem. Eng. Asp. 427 (2013) 76–82,
530 https://doi.org/10.1016/j.colsurfa.2013.03.030

531 [26] T. Saito, L. K Koopal, S. Nagasaki, S. Tanaka, Analysis of copper binding in the ternary
532 system Cu^{2+} humic acid/goethite at neutral to acidic pH, Environ. Sci. Technol. 39 (2005)
533 4886–4893, https://doi.org/10.1021/es0500308

534 [27] L. F Wang, L. L Wang, X. D. Ye, W. W Li, X. M Ren, G. P. Sheng, H. Q. Yu, X. K. Wang,
535 Coagulation Kinetics of Humic Aggregates in Mono- and Di-Valent Electrolyte Solutions,
536 Environ. Sci. Technol. 47 (10) (2013), https://doi.org/10.1021/es304993j

537 [28] Y. Yamashita, T. Saito, Effects of weak organic acids on the size distribution and size-
538 dependent metal binding of humic substances as studied by flow field-flow fractionation.
539 J. Environ. Chem. Eng. 3 (2015) 3024–3029, https://doi.org/10.1016/j.jece.2015.03.026

540 [29] M. Ishiguro, W. Tan, L K Koopal, Binding of cationic surfactants to humic substances,
541 Colloids Surfaces A Physicochem. Eng. Asp. 306 (2007) 29–39,
542 https://doi.org/10.1016/j.colsurfa.2006.12.024

543 [30] M. Kobayashi, Breakup and strength of polystyrene latex flocs subjected to a converging flow,
544 Colloids Surfaces A Physicochem. Eng. Asp. 235 (2004) 73–78.
545 https://doi.org/10.1016/j.colsurfa.2004.01.008

546 [31] P. Warszyński, G. Papastavrou, K. D. Wantke, H. Möhwald, Interpretation of adhesion force
547 between self-assembled monolayers measured by chemical force microscopy, Colloids
548 Surfaces A Physicochem. Eng. Asp. 214 (2003) 61–75, https://doi.org/10.1016/S0927-
549 7757(02)00362-X

550 [32] A. Noy, D. V. Vezenov, C. M. Lieber, Chemical force microscopy. Annu. Rev. Mater. Sci,
551 27 (1997) 381–421, https://doi.org/10.1146/annurev.matsci.27.1.381

552 [33] S. K. Sinniah, A. B. Steel, C J. Miller, J. E. Reutt-Robey, Solvent exclusion and chemical
553 constrast in scanning force microscopy, J. Am. Chem. Soc. 118 (1996) 8925–8931,
554 https://doi.org/10.1021/ja961295c

555 [34] D. V. Vezenov, A. Noy, L.F. Rozsnyai, C. M. Lieber, Force titrations and ionization state
556 sensitive imaging of functional groups in aqueous solutions by chemical force microscopy,
557 J. Am. Chem. Soc. 119(1997) 2006–2015. https://doi.org/10.1021/ja963375m

558 [35] N. Helfricht, E. Doblhofer, V. Bieber, P. Lommes, V. Sieber, T. Scheibel, G. Papastavrou,
559 Probing the adhesion properties of alginate hydrogels: a new approach towards the
560 preparation of soft colloidal probes for direct force measurements, Soft Matter 13 (2017)
561 578–589, https://doi.org/10.1039/c6sm02326f

562 [36] M. Brigante, G. Zanini, M. Avena, Effect of pH, anions and cations on the dissolution kinetics
563 of humic acid particles, Colloids and Surfaces A Physicochemical and Engineering Aspects
564 347 (2009) 180–186. https://doi.org/10.1016/j.colsurfa.2009.04.003

565 [37] M. Kobayashi, Strength of natural soil flocs. Water Res. 39 (2005) 3273–3278,
566 https://doi.org/10.1016/j.watres.2005.05.037

567 [38] A. Godec, K. Kogej, Binding of cetyl- and dodecylpyridinium cations by poly (L - glutamic
568 acid), Acta Chim. Slov. 54 (2007) 517–522

569 [39] J.J. Galán, A. González-Pérez, J.L. Del Castillo, J.R. Rodríguez, Thermal parameters
570 associated to micellization of dodecylpyridinium bromide and chloride in aqueous solution.
571 J. Therm. Anal. Calorim. 70 (2002), 229–234. https://doi.org/10.1023/A:1020678222376

572 [40] K. Heckmann, R. Schwarz, J. Strnad, Determination of Krafft point and CMC of
573 hexadecylpyridinium salts in electrolyte solutions. J. Colloid Interface Sci. 120 (1987)
574 114–117. https://doi.org/10.1016/0021-9797(87)90329-8

575 [41] Van Os, N.M., J.R. Haak, L.A.M. Rupert, Physico-Chemical Properties of Selected Anionic,
576 Cationic and Nonionic Surfactants, Physico-Chemical Properties of Selected Anionic,
577 Cationic and Nonionic Surfactants. Elsevier Science, 1993.

578 [42] P Sipos., P.M. May, G.T. Hefter, Carbonate removal from concentrated hydroxide solutions,
579 Analyst 125 (5) (2000) 955–958, https://doi.org/10.1039/A910335J

580 [43] S Blaser, Break-up of flocs in contraction and swirling flows, Colloids and Surfaces A, 166
581 (2000a) 215–223, https://doi.org/10.1016/S0927-7757(99)00450-1

582 [44] S. Blaser, Flocs in shear and strain flows, Journal of Colloid and Interface Science, 225
583 (2000b) 273–284, https://doi.org/10.1006/jcis.1999.6671

584 [45] K. Higashitani, N. Inada, T. Ochi, Floc breakup along centerline of contractile flow to orifice,
585 Colloids and Surfaces, 56 (1991) 13–23, https://doi.org/10.1016/0166-6622(91)80111-Z

586 [46] R. C. Sonntag, W. B. Russel, Structure and breakup of flocs subjected to fluid stresses: III.
587 Converging flow, Journal of Colloid and Interface Science, 115 (1987) 390–395,
588 https://doi.org/10.1016/0021-9797(87)90054-3

589 [47] S. Blaser, Forces on the surfaces of small ellipsoidal particles immersed in a linear flow field,
590 Chemical Engineering Science, 57(2002) 515–526, https://doi.org/10.1016/S0009-
591 2509(01)00389-X

592 [48] S. Moriguchi, Mathematical Formulas (Sugaku Koshikishu). Iwanami Shoten, Tokyo (in
593 Japanese), 1987

[49] J. F. L. Duval, K. I Wilkinson, H. P. Van Leeuwen, J. Buffle, Humic substances are soft and permeable: Evidence from their electrophoretic mobilities. Environ. Sci. Technol. 39(2005) 6435–6445, https://doi.org/10.1021/es050082x

[50] J.M. Cases, F. Villieras, Thermodynamic model of ionic and nonionic surfactants adsorption-abstraction on heterogeneous surfaces. Langmuir 8 (2005) 1251–1264. https://doi.org/10.1021/la00041a005

[51] J. Thieme, J. Niemeyer, Interaction of colloidal soil particles, humic substances and cationic detergents studied by X-ray microscopy. Struct. Dyn. Prop. Disperse Colloid. Syst. 2008, 193–201. https://doi.org/10.1007/bfb0118132

[52] F. Bouyer, A. Robben, W.L. Yu, M. Borkovec, Aggregation of colloidal particles in the presence of oppositely charged polyelectrolytes: Effect of surface charge heterogeneities. Langmuir 17(2001), 5225–5231. https://doi.org/10.1021/la010548z

[53] E. Illés, E. Tombácz, The effect of humic acid adsorption on pH-dependent surface charging and aggregation of magnetite nanoparticles. J. Colloid Interface Sci. 295 (2006),115–123. https://doi.org/10.1016/j.jcis.2005.08.003

[54] H. Hyung, J. H. Kim, Natural organic matter (NOM) adsorption to multi-walled carbon nanotubes: effect of NOM characteristics and water quality parameters, Environ. Sci. Technol 42 (2008) 4416–4421, https://doi.org/10.1021/es702916h

[55] A. Piccolo, 2001. the Supramolecular Structure of Humic Substances. Soil Sci. 166, 810–832. https://doi.org/10.1097/00010694-200111000-00007

[56] A. Hakim, M. Nishiya, M. Kobayashi, Charge reversal of sulfate latex induced by hydrophobic counterion: effects of surface charge density. Colloid Polym. Sci. 294 (2016) 1671–1678, https://doi.org/10.1007/s00396-016-3931-6

[57] T. Sugimoto, M. Nishiya, M. Kobayashi, Electrophoretic mobility of carboxyl latex particles: effects of hydrophobic monovalent counter-ions, Colloid. Polym. Sci. 295 (12) (2017) 2405–2411, http://dx.doi.org/10.1007/s00396-017-4219-1.

[58] N. Ryde, E. Matijevic, Kinetics of heterocoagulation. Part 4. Evaluation of absolute coagulation rate constant using a classical light scattering technique, Journal of Chemical Society, Faraday Transactions 90 (1994) 167–171, https://doi.org/ 10.1039/FT9949000167

[59] W. L. Yu, M. Borkovec, Distinguishing heteroaggregation from homoaggregation in mixed binary particle suspensions by multiangle static and dynamic light scattering. Journal of Physical Chemistry B 106 (2002) 13106–13110, https://doi.org/10.1021/jp021792h

[60] T. Shimizu, M. Seki, J. C. T. Kwak, The binding of cationic surfactants by hydrophobic alternating copolymers of maleic acid, Colloids and Surfaces 20 (1986) 289–301. https://doi.org/10.1016/0166-6622(86)80279-7

[61] T. Shimizu, J. C. T Kwak, The binding of cationic surfactants by hydrophobic alternating copolymers of maleic acid-charge density dependence, Colloids Surfaces A Physicochem. Eng. Asp. 82 (1994) 163-171, https://doi.org/10.1016/0927-7757(93)02642-R

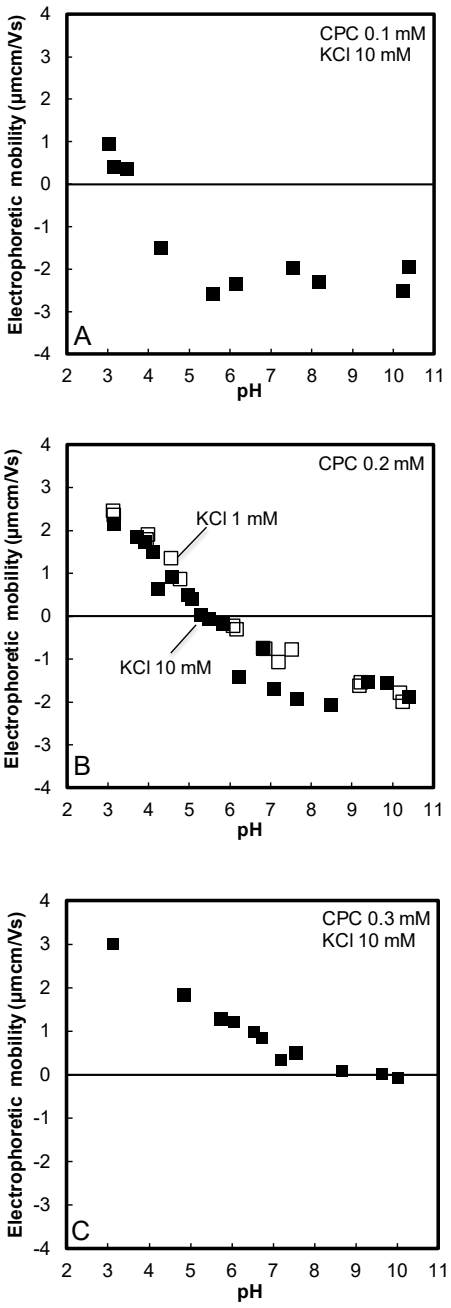

Figure 1. Electrophoretic mobility of Suwannee river fulvic acid (SRFA) at 0.1 mM (A), 0.2 mM (B), and 0.3 mM (C) CPC (cetylpyridinium chloride) as a function of pH. Concentration of SRFA is 50 mg/L.

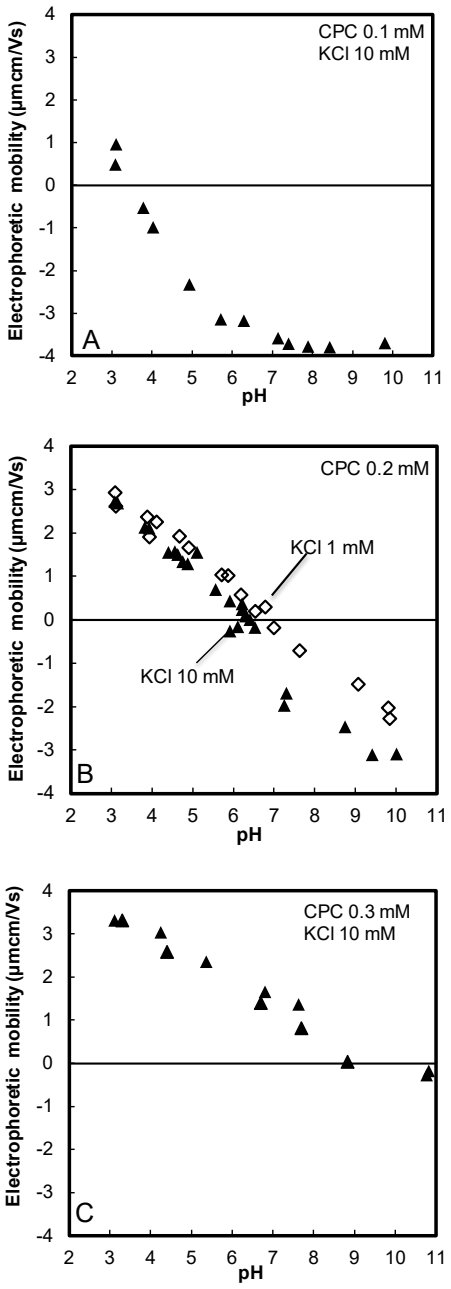

Figure 2. Electrophoretic mobility of Leonardite humic acid (LHA) at 0.1 mM, 0.2 mM, and 0.3 mM CPC (cetylpyridinium chloride) as a function of pH. Concentration of LHA is 50 mg/L.

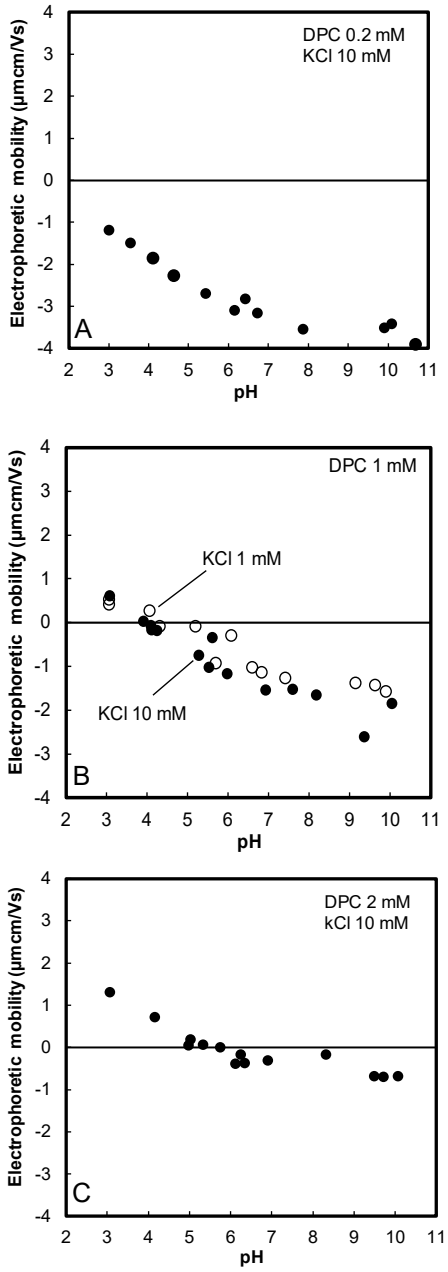

Figure 3. Electrophoretic mobility of Leonardite humic acid (LHA) at 0.2 mM (A), 1 mM (B), and 2 mM (C) DPC (dodecylpyridinium chloride) as a function of pH. Concentration of LHA is 50 mg/L.

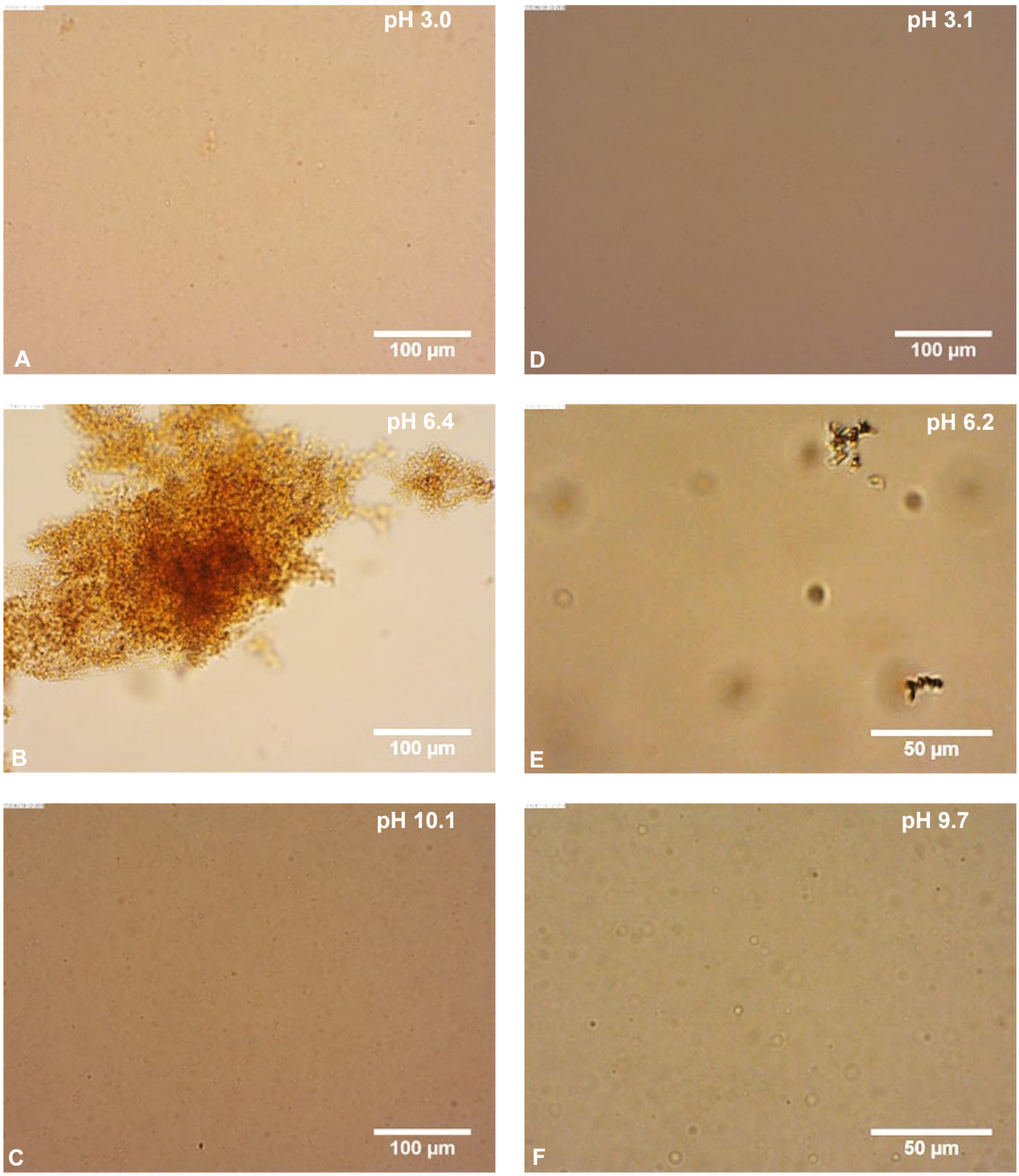

712 Figure 4. Microscopic images of Leonardite humic acid (LHA) in 0.2 mM CPC and KCl 10 mM
713 solution at pH 3 (A), 6.4 (B) and 10.1 (C) and Suwannee river fulvic acid (SRFA) in 0.2 mM CPC
714 and 10 mM KCl solution at pH 3.1, 6.2, and 9.7 (D, E, and F). Concentration of LHA and SRFA
715 is 50 mg/L. Brightness and contrast were corrected.

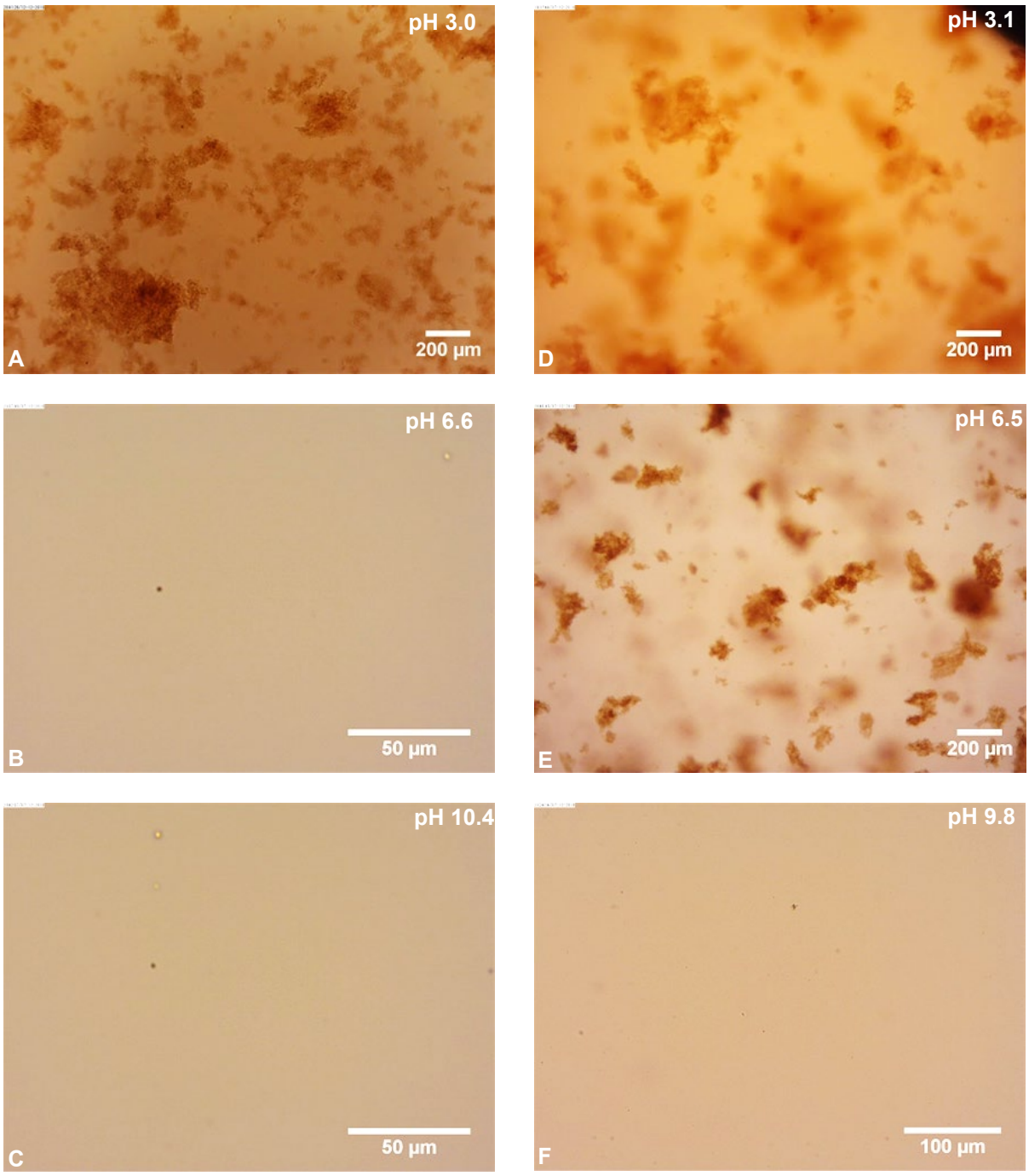

Figure 5. Microscopic images of Leonardite humic acid (LHA) in 0.2 mM DPC and KCl 10 mM solution at pH 3, 6.6 and10.4 (A, B, and C) and 1 mM DPC at 10 mM KCl solution at pH 3.1, 6.5, and 9.8 (D, E, and F). Concentration of LHA is 50 mg/L. Brightness and contrast were corrected.

716

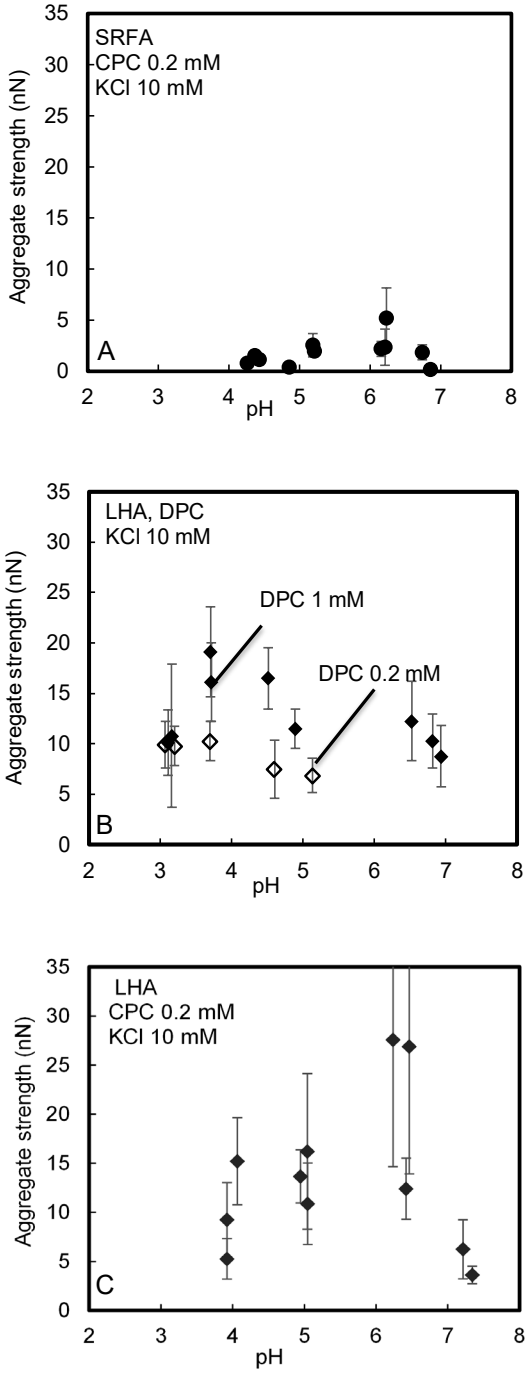

Figure 6. Aggregate strength of SRFA in 0.2 mM CPC at 10 mM KCl solution (A), LHA in 0.2 mM DPC and 1 mM DPC at 10 mM KCl solution (B) and LHA in 0.2 mM CPC at 10 mM KCl solution (C) as a function of pH. Concentration of LHA and SRFA are 50 mg/L.